Realization of an all-optical 2*4 decoder based on a two-dimensional photonic crystal

R. Arunkumar[1] · S. Robinson[1]

Abstract

Optical decoders are essentially required components for creating all-optical systems used in optical data processing and logical operations. In this paper, a novel structure of a 2*4 optical decoder is proposed for design using a two-dimensional photonic crystal (2D PhC). The proposed decoder is based on silicon rod photonic crystals with four output ports, two input ports, and a biasing port. For logic, 0 and 1 are introduced based on the maximum, and minimum power levels ($0.1P_{in}$ and $0.37P_{in}$), where P_{in} is the input power. Analyze of 2*4 decoder presented here is done using the Finite Difference Time Domain and Plane Wave Expansion methods—which provide the result of all functional parameter simulation and band structure of the lattice, respectively. The results show that the proposed 2*4 optical decoder with optimized functional parameters is suitable for all-optical information processing in future.

Keywords Two-dimensional photonic crystal · All-optical decoder · Photonic band gap · Optical beam

1 Introduction

Ultra-fast transmission speeds are among the goals of new communication network research. All communication activities in the network, including sending, receiving, and processing data, should take place fully optically. During the last few years, a new class of materials have emerged called photonic crystal (Joannopoulos et al. 1995), which provides capabilities along with new dimensions for controlling and manipulating light. Photonic Crystal nanostructures have low and high dielectric constants that alter electromagnetic wave propagation by alternately using low and high dielectric constant materials (Joannopoulos et al. 1995, 1997). The arrangement of periodic material in different axis, Photonic crystals can differ in one, two, and three dimensions. Photonic circuits are integrated using

✉ R. Arunkumar
  arunec002@gmail.com

  S. Robinson
  mail2robinson@gmail.com

1 Department of Electronic and Communication Engineering, Mount Zion College of Engineering and Technology, Pudukkottai, Tamil Nadu 622 507, India

materials like InP, GaAs, silicon on insulators and silicon. Here silicon has more attractive compared with other materials due to low losses and low thermal sensitivity (Joannopoulos et al. 2008).

One of the most fundamental characteristics of PhC is the Photonic Band Gap (PBG), which is used to change the confining of light at an optical wavelength, and the PBG has affected by creating defects in the form of cavities, waveguides, and resonatorsin a fundamental PhC structure (Alipour-Banaei et al. 2014a; Alipour-Banaei and Mehdizadeh 2013; Yi and Youn 2016). Due to their properties, these structures are better suited for designing and implementing fast optical devices, such as Sensor (Arunkumar et al. 2019a; Bahabady et al. 2017), Filters (Robinson and Nakkeeran 2013), Circulator (Arunkumar and Robinson 2021), Analog to digital converters (Youssefi et al. 2012), Multiplexer/Demultiplexer (Venkatachalam Rajarajan Balaji 2017), Power splitters (Arunkumar et al. 2019b), Adder/Subtractor (Neisy et al. 2018; Goswami et al. 2021), logical gates (Mondal et al. 2018; Ahmadi et al. 2023; Parandin et al. 2022; RamaPrabha and Robinson 2020), Isolator (Goswami et al. 2022, 2023), Encoder/Decoder (Arunkumar et al. 2022; Ebrahimi et al. 2022; Mohebzadeh-Bahabady and Olyaee 2020; Parandin 2019; Fallahi et al. 2021; Serajmohammadi and Alipour-Banaei 2014; Mehdizadeh et al. 2016; Mondal et al. 2019; Sharma 2022), etc.

The optical decoder is essential for all optical logic devices and computing applications (Rostamizadeh et al. 2020; Daghooghi et al. 2017; Aidinis, et al. , 2021; Maleki et al. 2020; Moniem 2015; Alipour-Banaei et al. 2014b; Mehdizadeh and Soroosh 2015; Mehdizadeh and Alipour-Banaei 2018; Daghooghi and Soroosh 2019; Askarian 2021; Askarian and Akbarizadeh, G". 2022; Fariborz Parandin et al. 2018; Khosravi and Zavvari 2018; Yasumoto 2006). The decoder consists of multiple input and output ports, and the output port's action is entirely based on the input port state and the biasing port state. While the multimode transmission, the single fiber and waveguides carry the multiple users probably communicate consequently, and the transmitted signal in a common medium is decoded at the receiver end. In several years, optical researchers have focused and endeavoured on all-optical decoders proposed.

A 2*4 decoder structure realized by Alidoost Rostamizadeh et al. The reported decoder designed by cascading the 3 optical switches made up of non linear rods whose refractive index and Kerr coefficient are 1.4 and 10–14 m^2/W. The footprint of the structure is about 861 µm^2 (Rostamizadeh et al. 2020). Tina Daghooghi et al. proposed the 2*4 decoder optical switch which investigated using the 31×31 cubic lattice structure. Six different ring resonator introduced into the waveguide. The operational speed of the decoder is 160 GHz. The functional parameters such as Insertion loss and cross talk calculated as—20 dB (Daghooghi et al. 2017). The 1*2 decoder designed using the Self-collimated Beam Method in 2D Photonic Crystals. The functional parameters such as a Contrast ratio of 2.02 dB and abit rate of 2.8 Tb/s are investigated by Konstantinos Aidinis et al. (Aidinis, et al. , 2021). M. J. Maleki et al. reported the all-optical 2-to-4 decoder by introducing the three optical cavities with non-linear rods using Kerr coefficient of 10^{-14} m^2/W (Maleki et al. 2020). Moniem proposed a 2*4 decoder structure using a combination of five nonlinear photonic crystal ring resonator with T shaped waveguide. These devices consist of two 1*2 decoder to operate as a 4*2 decoder and they have obtained the functional parameters such as cross talk and insertion loss of − 10 dB and − 8.8 dB respectively (Moniem 2015). Askarian et al. has been proposed the all optical 2×4 decoder and the device is estimated the functional parameter in which the delay time, cross section, and contrast ratio were about 2 ps, 420 µm 2 and 7.73 dB, respectively (Askarian 2021). Fariborz Parandin et al. realized the X shaped 1*2 decoder with low compact in size and the functional parameters investigated as bit rate and time delay of 2Tbit/s and 0.1 ps respectively (Fariborz Parandin et al. 2018).

From the above literature analysis it is clearly noticed that there are several attempts made in optimization of decoder in photonic crystal still many of the structural design contain low efficiency and the size of the structure will be too large. Initially it is investigated that most of the decoder constructed using the ring resonator based structure. Meanwhile using the ring resonator structure the power coupled inside the resonator and there will be a maximum amount of power loss inside the structure is identified, therefore the output efficiency obtained as low. Typically few functional parameters calculated from all the reported decoder.

The proposed design of the decoder is typically used to convert 'n' input signals into '2n' output signals uniformly. In the conventional design, a 2*4 decoder is used, and its functional parameters are accounted for. The proposed design was constructed using a line and point defect-based structure with high efficiency to enhance device performance and mitigate the issues reported in previous decoders. A nanocavity is incorporated in the waveguide to decrease leakage power at resonance, which lowers the leakage power and boosts output power. The proposed design uses Plane Wave Expansion (PWE) and Finite Difference Time Domain (FDTD) to examine the spectrum and band gap. Additionally, six more functional parameters are investigated, showing better performance compared to all other reported decoders, including response time, bit rate, steady-state time, insertion loss, crosstalk, and contrast ratio. Therefore, the proposed structure is more suitable for photonic integrated optical circuits and high-speed switching systems.

The rest of the paper is organized as follows: Section II describes the structural design and optimization of Photonic Crystal based 2*4 decoder are presented, Section III describes the results and discussion of the proposed structure and Section IV concludes the proposed work.

2 Design and optimization of Photonic Crystal based 2*4 decoder

This section's purpose is to describe and design the proposed 2*4 decoder. Figure 1, shows that the decoder is a combinational logic circuit used to change the code into a set of the signal. A decoder circuit takes multiple outputs. The decoder binary data is 'n' input into '2^n' output.

The block diagram of the 2*4 line decoder is shown in Fig. 1 Port A and B are the two inputs, where O_1, O_2, O_3, and O_4 are the four outputs. The truth table explains the
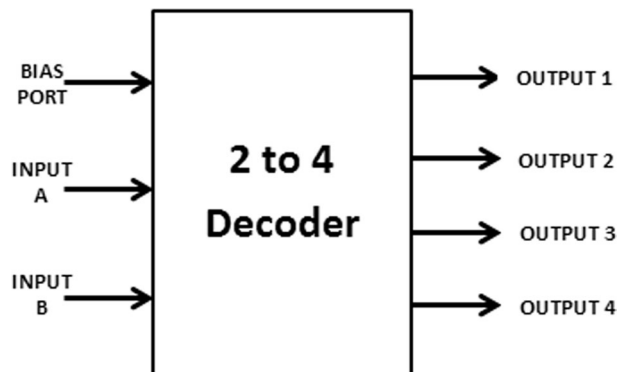

Fig. 1 Block diagram of 2*4 decoder

Table 1 Truth Table for 2*4 decoder

Input		Output			
A	B	O_1	O_2	O_3	O_4
0	0	1	0	0	0
0	1	0	1	0	0
1	0	0	0	1	0
1	1	0	0	0	1

operations of a 2*4decoder in Table 1., The binary inputs A and B determine which output line from O_1 to O_4 is "HIGH" at logical level "1" while the remaining outputs are maintained "LOW" at logic0.Therefore, whichever output line is "HIGH" identifies the binary code present at the input, in other words it "decodes" the binary input. Some binary decoders have an additional input pin labeled "Enable" that controls the outputs from the device.

First, a gap map is used to select the structural parameters of the proposed device, such as the rod's radius, the lattice constant, and the materials' refractive indices. Changing the structural parameters allows the gap map to generally offer a variation of TE/TM PBG. The refractive index difference, defect size, rod radius, and lattice constant variations were used to create the gap map in Fig. 2a–c, which depict variations in TE/TM PBG. In these diagrams, the red zone represents the TM PBG, while the blue region shows how the TE PBG varies about the rods' radius, period, and delta.

The TE BPG section of the structure is shown by the vertical yellow line crossing the blue region without adding any faults. The structural design uses a gap map to identify the appropriate structural parameter such as radius, refractive index and lattice constant. Through the gap map, the following values, such as a radius of 100 nm, a lattice constant of 550 nm and a refractive index of 3.47, are selected based on these values the photonic band gap will be fixed in the proposed work. Due to this gap map selection, the PBG wavelength is set and it can be enhanced to work in third generation optical window.

The fundamental structure of the proposed 2*4 decoder is a 39×25square array lattice of circular silica rods with the refractive index of 3.47 in back round of air medium. We have manipulated the PWE (plane wave expansion) technique to examine the proposed design's functional parameters to calculate the structure band gap. Figure 3 shows the calculation of the band diagram for the proposed 2*4 Decoder. It depicts mode(TM/TE) propagation inside the PC and is determined by PWE. Figure 3 shows two different PBG in the TE mode for the structure. The structure includes the band gap in the TE mode 1 is $0.3 < a/\lambda < 0.44$ and TE mode 2 is $0.73 < a/\lambda < 0.75$, which corresponds to the wavelength $1250 < \lambda < 1833$ and $733 < \lambda < 753$, respectively. From the analysis of the band gap for the 2*4 Decoder, the TE mode 1 can be comprehended that the band gap is suitable for the third-generation optical window for optical communication systems.

Figure 4, shows the 3D view for the proposed 2*4 decoder and it depicts the footprint of the proposed design. The 3D structure of the 2D PC based 2*4 decoder includes the footprint dimension in X axis 13.8 μm and Z axis 21.4 μm and the surface area of the design is $295 \mu m^2$ estimated.

For implementing the proposed structure of the 2*4 decoder, the new square lattice design with line and point defect of structure along with linear optical waveguides are utilized with the same parameter. The performance characteristics of the device, such as output power response time, contrast ratio, and bit rate, can be improved by optimizing the radius of the nano cavity. To achieve this, the nano cavity's rod radius is chosen to be either

Fig. 2 Effect of gapmap by varying) Radius of the rod, **b** Period (Lattice constant) and **c** Delta (Index contrast)
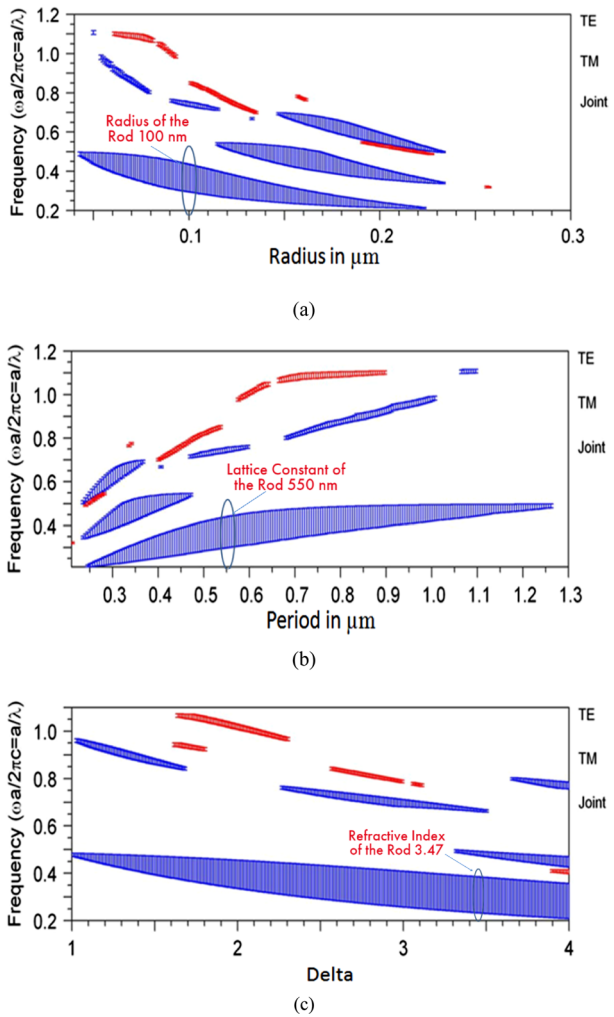

(a)

(b)

(c)

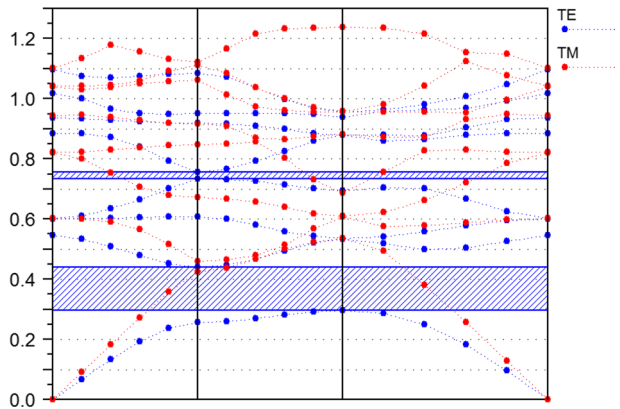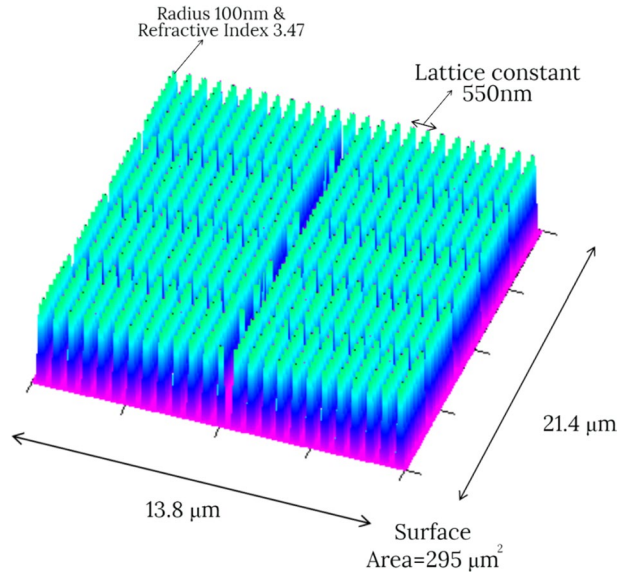**Fig. 3** Fundamental structure of 2*4 decoder

Fig. 4 3D structure of 2*4 decoder design

Radius 100nm & Refractive Index 3.47

Lattice constant 550nm

21.4 μm

13.8 μm

Surface Area=295 μm^2

50 nm or 100 nm. Typically, the rod's radius is altered between 30 and 115 nm to determine the optimal size for the nano cavity. Figures 5 and 6 present the effects of altering the rod radius on the normalized power. Based on these data, the rod radius of 50 nm and 100 nm are selected for further analysis of logical conduction and functional parameters calculation.

Figure 7 shows that the 2*4 decoder structure consists of 39×25 an array of dielectric rods and the radius of the dielectric rods is used in the proposed design is 0.1 μm and
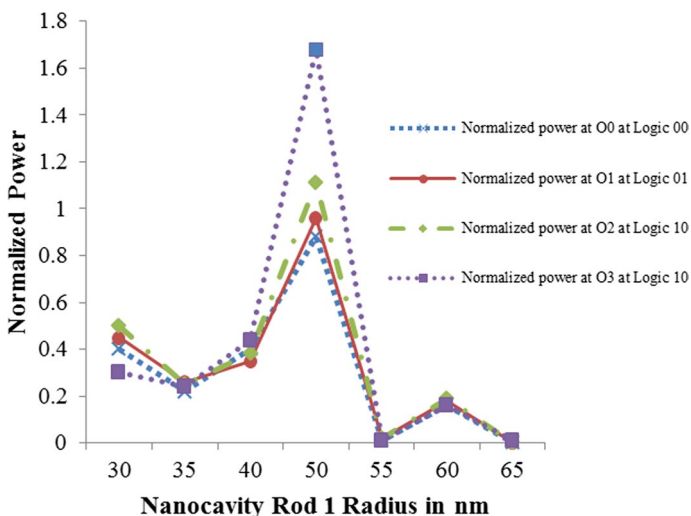

Fig. 5 Normalized power for different rod 1 radius for all logic in Decoder
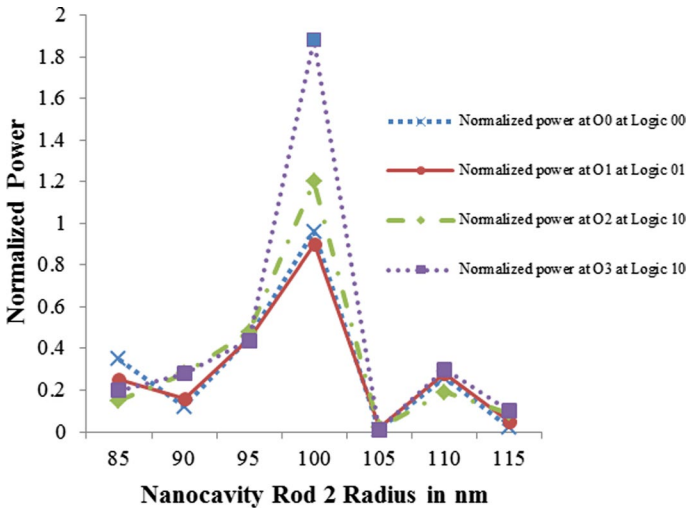
Fig. 6 Normalized power for different inner rod2 radius for all logic in Decoder
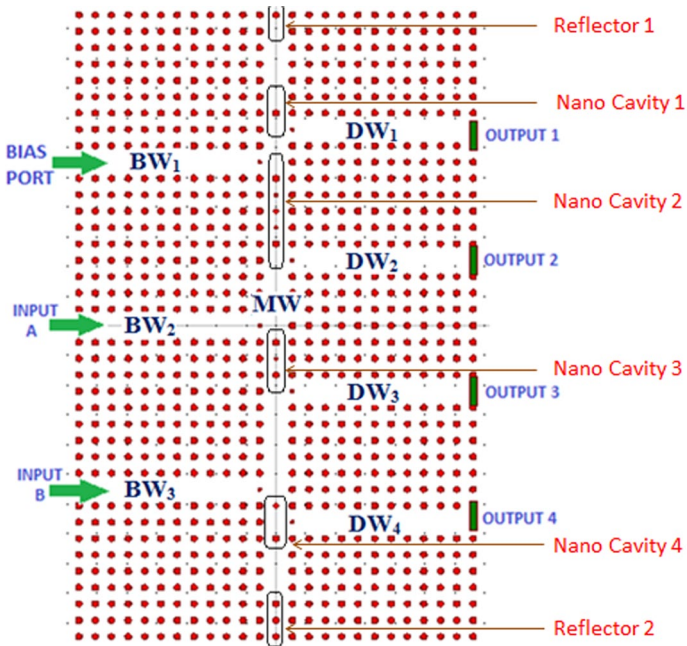

Fig. 7 Proposed structure of 2*4 decoder

0.05 µm. The proposed decoder is designed using a square lattice which is easy to make the bus and drop waveguides and create the nano resonant cavity in the waveguides.

The optical decoder generates 'n' input into '2^n' output, and there will only ever be one active output line for each input signal A and B. The decoder consists of two input linear

bus waveguides named by input ports A and B, one bias linear bias waveguide respectively BW_1, BW_2, and BW_3, four linear drop waveguides DW_1, DW_2, DW_3 and DW_4 for the output O_1, O_2, O_3, and O_4. The drop and Bus waveguides are created by removing the 11 dielectric rods in the respective axis. The operating wavelength of the proposed design 1550 nm Gaussian signal propagates through the bus and drop waveguide to enhance the logic of the decoder.

The Four nano resonant cavities (NRC), which is the primary element in the decoder, are designed using point defects. Four NRC are place in the middle waveguide (MW). The NRC in the proposed design improves the coupling between the input and the output optical signal and increases the transmission efficiency of the resonant wavelength. From the input waveguide, the respective logic is applied and the NRC couple the Gaussian signal and the same coupled signal reach the drop waveguide to enable the respective logic.

3 Results and discussion

In this section, we present the simulation results of the final proposed structure using the FDTD method. In this simulation, four different input states are applied with altered combinations of two inputs, A and B, and the bias port is in the ON condition when A and B are in the OFF state. The proposed structure is simulated using an operating wavelength of 1550 nm. As shown in Fig. 8, the optical intensities of the input signals are set to 1mW. If the power of the input signal is increased above the switching threshold of the nanocavity for this structure (1mW), the resonant wavelength of the structure is not coupled to the output ports O1, O2, O3, and O4. The normalized power variation of the output ports versus the input power of the respective port is more than 90% in the ON state and less than 10% in the OFF state. Additionally, functional parameters such as bit rate, delay time, and contrast ratio are examined for the Decoder.
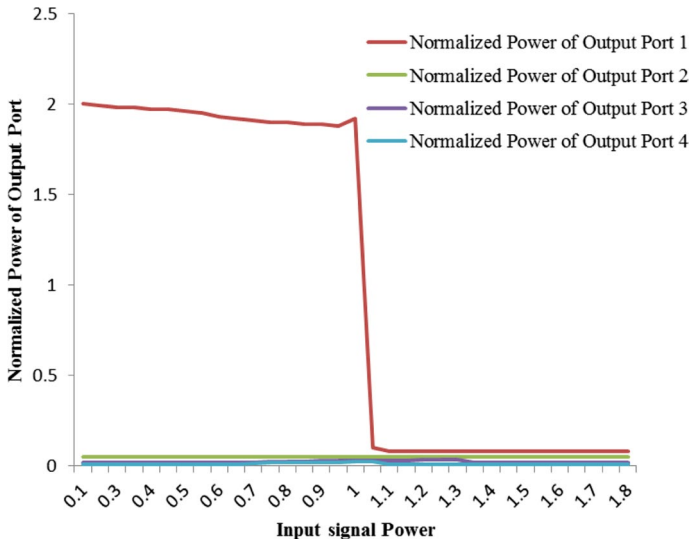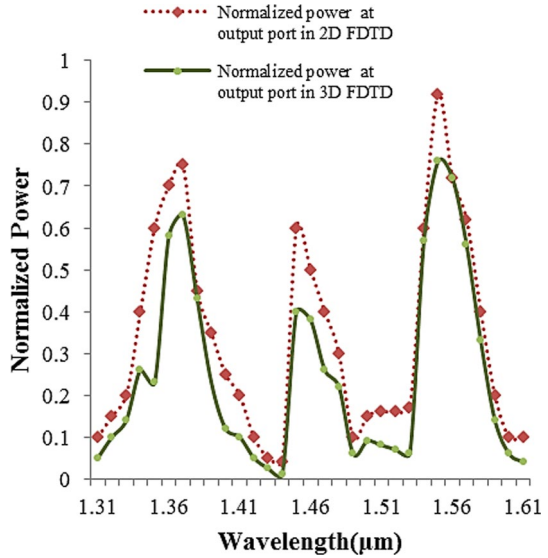

Fig. 8 Variation normalized power at output power versus input power

Fig. 9 Comparison of Normalized power at output port in 2D FDTD and 3D FDTD

The proposed decoder is simulated using both 3D FDTD and 2D FDTD. The input light signal is launched in the input bias port, and the output power is observed in the output port. The corresponding response curve is depicted in the Fig. 9, showing several distinct resonant peaks in this wavelength with different normalized powers. The 2D FDTD and 3D FDTD both provide the same simulation results and similar output response, although 3D FDTD offers a slightly better response. However, the time taken for simulation is too high compared to 2D FDTD. Hence, the authors preferred the 2D FDTD method for simulation in the proposed decoder, and various functional parameters are investigated.

Case 1 When both A and B are OFF and Bias port is in ON condition, according to the state, the optical beam is coming from the Bias port and propagates inside the linear bus waveguides BW_1. Therefore all the linear waveguides become no propagation of optical waves. Figure 10a shows the field distribution diagram for the input state (0, 0). In this case, optical signals propagate from input to output through drop DW_1 linear waveguides, and no optical waves propagate toward DW_2, DW_3 and DW_4. As a result, in this case, O_1 is ON, and the other ports are OFF (Fig. 10a). As shown in Fig. 10a, the normalized Power at O_1 is about 0.88 P_{in} but the optical power at the other ports is less than 0.01 P_{in}.

Case 2 For the input of (0,1), When both A and Bias are OFF, and Input port B is in ON condition, according to the state, the optical beam is coming from the input port B and propagates inside the linear bus waveguides BW_2. In this case, optical signals propagate from input to output through drop DW_2 linear waveguides, and no optical waves propagate toward DW_1, DW_3 and DW_4. As a result, in this case, output port O_2 is in an ON state, and the other port is in OFF (Fig. 10b). As shown in Fig. 10b, the normalized Power at O_2 is about 0.88 P_{in} but the optical power at the other ports is less than 0.01 P_{in}.

Case 3 When A = 1 and Bias = B = 0, the output signal appears at the O_3. All other ports are inactive in this state, and the output signal appears in O_3 through the DW_3 drop waveguide. Nano coupling rods are used to couple the input signal to the linear waveguide W_3 at the resonant wavelength and achieve maximum output power. Figure 10c indicates that the normalized output power of 1.11 P_{in} reaches O_3.
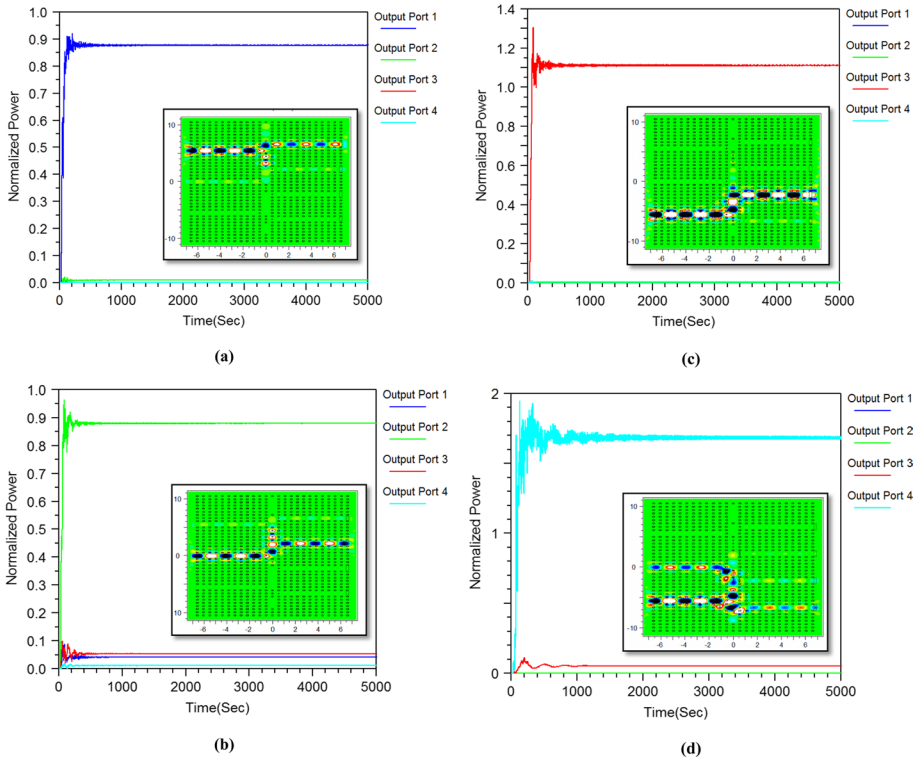
Fig. 10 Field distribution and Pulse response of the proposed structure in response to the states **a** AB = 00 & E = 1, **b** AB = 01& E = 0, **c** AB = 10 & E = 0, **d** AB = 11& E = 0

Case 4 Finally, as shown in Fig. 10d, in the last case, both logic ports are ON (A = B = 1), and Bias port is in the active state. In this case, the resonant due to the presence of optical power near nano coupling rods is increased the coupling effect to input bus waveguide BW_2 and BW_3 and linear drop waveguide DW_4. Therefore, the input signal propagates toward the O4 port and turns it ON (O4 = 1), and the other three ports are in OFF state. Figure 10d shows the normalized signal logic's power observed in the output port at 1.68 P_{in}.

It is also necessary to conduct other analyses besides electric field distribution. A common challenge in integrating optical devices is the power levels of logic 0 and 1. Time and power analyses are conducted to evaluate the proposed structure's suitability for use in integrated optical circuits, and the results are shown in Fig. 10a–d. In Table 2 the details of these diagrams are collected for a better understanding of the logical state of the input ports, the standardized intensity, and the logical state of output ports. According to Table 2, the proposed optical structure can be demonstrated as an all-optical decoder 2*4 in comparison with a conventional decoder 2*4.

The other main parameters of the multiple port all-optical decoder, including delay time, response time, steady state time, bit rate, contrast ratio, cross-talk and insertion loss, should be carefully calculated.

Table 2 Output power level of 2*4 Decoder Design

Inputs		Outputs							
I_1	I_2	O_0		O_1		O_2		O_3	
		Logic	Normalized power in %	Logic	Normalized power in %	Logic	Normalized power in %	Logic	Normalized power in %
0	0	1	$0.88P_{in}$	0	$0.01\ P_{in}$	0	$0.0001\ P_{in}$	0	$0.0001\ P_{in}$
0	1	0	$0.0004\ P_{in}$	1	$0.88\ P_{in}$	0	$0.0005\ P_{in}$	0	$0.01\ P_{in}$
1	0	0	0	0	$0.05\ P_{in}$	1	$1.11\ P_{in}$	0	$0.01\ P_{in}$
1	1	0	0	0	0	0	$0.05\ P_{in}$	1	$1.68\ P_{in}$

3.1 Contrast ratio

The contrast ratio, defined as 10log (Plogic1/Plogic0), indicates the power margin between logics 1 and 0.

3.2 Insertion loss

The optical insertion loss is one of the most challenging characteristics for low-power devices which is defined by 10log ((Pin-Pout)/Pin).

3.3 Cross-talk

The other dominant parameter in multiple port optical devices is cross-talk, which shows the effects of ports on each other and defined as 10log (P_{low}/P_{high}) where P_{low} and P_{high} are the lowest and the highest power levels obtained at output ports for each logic state.

3.4 Response time

Here the response time is calculated by the difference between the time taken for 10% of normalized power and 90% of normalized power.

Table 3 The calculated characteristics of the proposed decoder

Logic	Delay time in ps	Response time in ps	Steady state time in ps	Bit rate in Tbps	Contrast ratio in dB	Crosstalk in dB	Insertion loss in dB
00	0.2	0.8	1.09	1.25	22.4	− 19.52	− 9.13
01	0.14	0.47	1.03	2.12		− 18.1	0
10	0.17	0.35	1.66	2.85		− 21.4	0
11	0.19	0.34	3.54	2.95		− 15.17	0

3.5 Bit rate

The bit rate is referred to the speed at which data is transferred and can be calculated using the time response of the output signal. The bit rate is the reciprocal of the response time.

The characteristics mentioned above are reported in Table 3. As it can be concluded, the contrast ratio of the proposed decoder is about 22.4 dB and the insertion loss is varied from − 9.13 dB to 0. The maximum cross-talk is between − 15.17 and − 21.4 dB. Since the maximum steady-state time of the decoder is about 3.54 ps. So, the maximum bit rate is calculated at about 2.95Tbps. It can be concluded that the proposed decoder is potentially applicable in real-time implementations.

Table 4 compares the performance metrics of the suggested optical decoder to those of other optical decoders. The comparison includes the lattice of the structure, footprint, defects, delay time, response time, steady state time, bit rate, contrast ratio, crosstalk, and insertion loss of the proposed structure. As the proposed structure uses line and point defect-based resonant cavities, the total footprint of this optical structure, which is 295 µm2, is smaller than all previously designed structures. In addition, the proposed optical decoder uses a significantly lower input power (1 mW), has a lower delay time (0.14 ps), and a faster response time (0.34 ps) than previous works. Furthermore, the proposed optical decoder was designed with a high contrast ratio (22.4 dB), a high bit rate (2.95 Tbps), an acceptable insertion loss (− 9.13 dB), low crosstalk (21.4 dB), and steady-state response (1.03 ps). From the above comparison of functional parameters, it is clear that in some previously reported works, the contrast ratio decreased as the response time increased. At the same time, if the contrast ratio was better, then the bit rate, insertion loss, and steady-state time were minimal and not calculated in the reported work. Typically, in the above-reported works, not all functional parameters were investigated. In contrast to previously reported decoders, the proposed decoder investigated all functional parameters and showed significant improvement in all parameters while also having a smaller size. Therefore, the proposed decoder is well-suited for use in photonic integrated circuits for high-speed computing.

3.6 Fabrication techniques

By using an SOI wafer, the PC-based proposed 2*4 Decoder is produced. The SOI wafer is created using a stack of Si-SiO$_2$-Si material with thicknesses of 200 nm, 1000 nm, and 450 nm. Once the SOI has been produced, the wafer is spin-coated with a 100 nm thick layer of PMMA resist material at 7000 rpm for 15 min. Figure 11 depicts the fabrication flow process of Pillar type PC devices.

After the SOI substrate is formed, a 100 nm layer of polymethyl methacrylate (PMMA) resist material is spin-coated over it for 15 min at 7000 rpm. The mask pattern for the SOI substrate is then created using PMMA. The CleWin 4.1 layout editor was used to create this mask pattern. Before the lithography process, the PMMA resist undergoes a soft bake at 110 °C for 10 min. Once the procedure is complete, the wafer is ready for lithography. Various lithography methods, such as optical, electron beam, and focused ion beam lithography, can be used during fabrication. The proposed design requires E-Beam Lithography due to its precise vertical etching for a few tens of nanometers. The Raith E-line direct electron beam lithography system is ideal for this purpose because it offers ultra-high resolution, a maximum acceleration voltage of up to 30 kV, and nano manipulators to obtain

Table 4 Comparison of the proposed structure with previous optical decoders

| References	Lattice	Footprint in μm^2	Mechanism	Delay Time in ps	Response Time in ps	Steady-state time in ps	Bit Rate in Tbps	Contrast Ratio in dB	Crosstalk in dB	Insertion Loss in dB
Rostamizadeh et al. (2020)	Cubic/Square	861	Ring Resonator & Line and Point defect	**	**	**	**	10.6	**	**
Daghooghi et al. (2017)	Cubic/Square	512	Ring Resonator	**	**	6	0.16	**	−15.6	−20
Maleki et al. (2020)	Cubic/Triangular	110	Line and Point defect	**	**	1	1	13.42	**	**
Moniem (2015)	Cubic/Square	1520	Ring Resonator & Line and Point defect	**	**	3.83	0.2	**	**	**
Alipour-Banaei et al. (2014b)	Cubic/Square	1905	Ring Resonator	**	**	**	**	**	**	**
Mehdizadeh and Soroosh (2015)	Cubic/Triangular	1513	Ring Resonator	**	**	**	**	**	**	**
Mehdizadeh and Alipour-Banaei (2018)	Cubic/Square	581	Ring Resonator	**	**	10	0.01	**	**	**
Daghooghi and Soroosh (2019)	Cubic/Square	437	Ring Resonator & Line and Point defect	4.5	**	**	0.22	13.42	−16.38	−7.45
Askarian (2021)	Cubic/Triangular	420	Ring Resonator & Line and Point defect	2	**	**	0.5	10.58	**	**
Askarian and Akbarizadeh, Gʼʼ. (2022)	Cubic/Triangular	561	Ring Resonator	2	**	**	0.5	9.32	**	**
This work	Cubic/Square	295	Line and Point defect	0.14	0.34	1.03	2.95	22.4	−21.4	−9.13
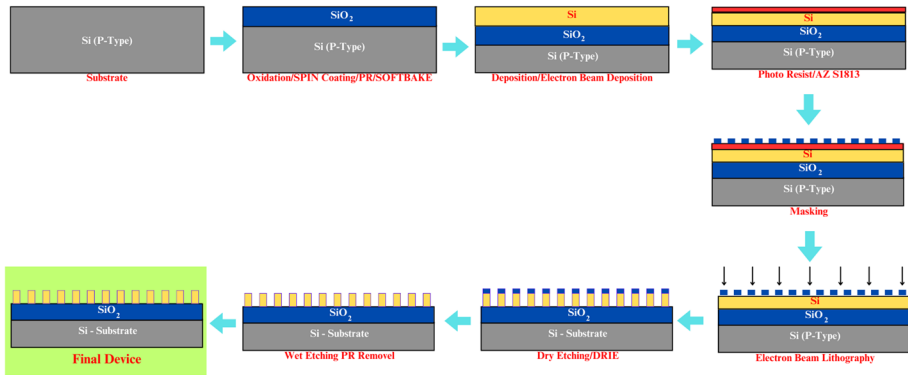
Fig. 11 Fabrication processes of Pillar type PC devices

the pattern of the air hole structure. Other techniques cannot control feature sizes in subnanometer sizes. To dehydrate the produced substrate, it is then heated to 180 °C.

Using the masking pattern, an array of pillars is formed via deep vertical dry etching or deep reactive ion etching (DRIE). The SiO_2 oxide layer is then removed using a wet etching procedure, followed by a 16-min BHF acid washing. The SiO_2 oxide layer serves as a sacrifice layer to suspend the PC in the air. As mentioned earlier, the fabrication will make the PC-based Decoder possible.

4 Conclusion

In this attempt, the 2*4 all-optical decoder is invented by arrangement based on line and point defects of silicon rods with background air substrate. We can switch among four different output ports in the proposed structure by using two logic input ports. We used linear waveguides W1, W2, W3 and W4 for designing the decoder. The resonant wavelength of the proposed design is 1550 nm. The output characteristics such as delay time, response time, contrast ratio, cross-talk, steady-state, bit rate and insertion loss are estimated as 0.14 ps,0.34 ps, 22.4 dB, − 21.4 dB, 3.54 ps, 2.95Tbps and − 9.13 dB respectively. The footprint of the proposed design is 295μm². According to all reported results, the proposed all-optical decoder can be highly suitable for all-optical integrated communication systems and optical information processing systems.

Author contributions All Authors are responsible for the correctness of the statements provided in the manuscript. The following contributions have been made by the Authors. RA is calculated the structural parameters, such as, radius of the rod, lattice constant and refractive index, designed and simulated the proposed 2×4 Decoder. The electric field distribution, output response, bit rate, contrast ratio, response time is analyzed by RA. SR is given the idea, verify the all the simulated results and corrected the manuscript. Authors read and approved the final manuscript.

Declarations

References

Ahmadi, A., Veisi, E., Ehyaee, A., Seifouri, M., Olyaee, S.: Design of a compact polarization-independent all-optical and logic gate based on silicon photonic crystal. SILICON (2023). https://doi.org/10.1007/s12633-023-02334-5

Aidinis, K., et al.: All-optical 1×2 decoder based on the self-collimated beam method in 2D photonic crystals. Photon. Nanostruct. Fundam. Appl. **43**, 10080 (2021)

Alipour-Banaei, H., Mehdizadeh, F.: Band gap calculation of 2D hexagonal photonic crystal structures based on regression analysis. J. Opt. Commun. **34**, 1–9 (2013)

Alipour-Banaei, H., Serajmohammadi, S., Mehdizadeh, F.: A band gap properties of two-dimensional photonic crystal structures with rectangular lattice. J. Opt. Commun. **36**, 1–7 (2014a)

Alipour-Banaei, H., Mehdizadeh, F., Serajmohammadi, S., Hassangholizadeh-Kashtiban, M.: A 2*4 all optical decoder switch based on photonic crystal ring resonators. J. Mod. Opt. **62**, 430–434 (2014b)

Arunkumar, R., Robinson, S.: Investigation on ultra-compact 2D-PC based optical circulator for photonic integrated circuits. J. Optoelectron. Adv. Mater. **23**, 112–118 (2021)

Arunkumar, R., Suaganya, T., Robinson, S.: Design and analysis of 2D photonic crystal based biosensor to detect different blood components. Photon. Sens. **9**, 69–77 (2019a)

Arunkumar, R., Jayabarathan, J.K., Robinson, S.: Design and analysis of optical Y-splitters based on two-dimensional photonic crystal ring resonator. J. Optoelectron. Adv. Mater. **21**(7–8), 435–442 (2019b)

Arunkumar, R., Kavitha, V., Rama Prabha, K., et al.: Investigation on ultra-compact, high contrast ratio 2D-photonic crystal based all optical 4×2 encoder. Opt. Quant. Electron. **54**, 110 (2022)

Askarian, A.: Design and analysis of all optical 2×4 decoder based on kerr effect and beams interference procedure. Opt. Quant. Electron. **53**(291), 1–17 (2021)

Askarian, A., Akbarizadeh, G.: A novel proposal for all optical 2×4 decoder based on photonic crystal and threshold switching method. Opt. Quant. Electron. **54**(84), 1–15 (2022)

Bahabady, A.M., Olyaee, S., Arman, H.: Optical biochemical sensor using photonic crystal nano-ring resonators for the detection of protein concentration. Curr. Nanosci. **13**(4), 421–425 (2017)

Balaji, V.R., Murugan, M., Robinson, S., Nakkeeran, R.: Design and optimization of photonic crystal based eight channel dense wavelength division multiplexing demultiplexer using conjugate radiant neural network. J. Opt. Quant. Electron. **49**(198), 1–15 (2017)

Daghooghi, T., Soroosh, M.: Slow light in ultra-compact photonic crystal decoder. Appl. Opt. **58**, 2050–2057 (2019)

Daghooghi, T., Soroosh, M., Ansari-Asl, K.: A novel proposal for all-optical decoder based on photonic crystals. Photonic Netw. Commun. **35**, 335–341 (2017)

Ebrahimi, V., Fallahi, V., Olyaee, S., et al.: Design, simulation and optimization of an ultracompact all-optical encoder based on 2D-PC. Opt. Quant. Electron. **54**, 643 (2022). https://doi.org/10.1007/s11082-022-04060-5

Fallahi, V., Mohammadi, M., Kordrostami, Z., et al.: Design and optimization of an ultra-fast symmetrical 4 $\times$ 2 encoder based on 2D photonic crystal nano-resonators for integrated optical circuits. Opt. Quant. Electron. **53**, 574 (2021). https://doi.org/10.1007/s11082-021-03195-1

Goswami, K., Mondal, H., Sen, M.: A review on all-optical logic adder: Heading towards next-generation processor. Opt. Commun. **483**, 126668 (2021)

Goswami, K., Mondal, H., Sen, M.: Optimized design of multiple bends for maximum power transfer in optical waveguide. Optik **265**, 169448 (2022)

Goswami, K., Mondal, H., Sen, M.: Design and analysis of passive and phase insensitive all-optical isolator in linear optical platform. Opt. Commun. **529**, 129071 (2023)

Joannopoulos, J.D., Winn, J.N., Mead, R.D.: Photonic Crystals: Molding the Flow of Light. Princeton Press, Princeton (1995)

Joannopoulos, J.D., Villeneuve, P.R., Fan, S.: Photonic crystals: putting a new twist on light. J. Nat. **386**, 143–149 (1997)

Joannopoulos, D.J., StevenJohnson, G., Winn, N.J., Meade, R.D.: Photonic Crystals: Modeling the Flow of Light, 2nd edn. Princeton University Press (2008)

Khosravi, S., Zavvari, M.: Design and analysis of integrated all-optical 2×4 decoder based on 2D photonic crystals. Photonic Netw. Commun. **35**(1), 122–128 (2018). https://doi.org/10.1007/s11107-017-0724-x

Maleki, M.J., Soroosh, M., Mir, A.: Ultra-fast all-optical 2-to-4 decoder based on a photonic crystal structure. Appl. Opt. **59**(18), 5422–5428 (2020)

Mehdizadeh, F., Alipour-Banaei, H.: Design and simulation of all optical decoder based on nonlinear PhCRRs". Opt. Int. J. Light Electron Opt. **156**, 701–706 (2018)

Mehdizadeh, F., Soroosh, M.: A novel proposal for optical decoder switch based on photonic crystal ring resonators. Opt. Quantum Electron. **48**, 20–28 (2015)

Mehdizadeh, F., Soroosh, M., Alipour-Banaei, H., Alipour-Banaei, A., Mahdizadeh, F., Serajmohammadi, S.: A novel proposal for optical decoder switch based on photonic crystal ring resonators. Opt. Quant. Electron. **48**(20), 1–9 (2016)

Mohebzadeh-Bahabady, A., Olyaee, S.: Designing an ultracompact all-optical 4-to-2 encoder and investigating its optical power consumption. Appl. Opt. **59**, 2409–2415 (2020)

Mondal, H., Sen, M., Prakash, C., Goswami, K., Sarma, C.K.: Impedance matching theory to design an all-optical AND gate". IET Optoelectron. **12**(5), 244–248 (2018)

Mondal, H., Sen, M., Goswami, K.: Design and analysis of all-optical 1-to-2 line decoder based on linear photonic crystal. IET Optoelectronic. **13**, 191–195 (2019). https://doi.org/10.1049/iet-opt.2018.5099

Moniem, T.A.: All optical active high decoder using integrated 2D square lattice photonic crystal. J. Mod. Opt. **62**, 1643–1649 (2015)

Neisy, M., Soroosh, M., Ansari-Asl, K.: All optical half adder based on photonic crystal resonant cavities. J. Photon Netw. Commun. **35**(2), 245–250 (2018)

Parandin, F.: High contrast ratio all-optical 4 × 2 encoder based on two-dimensional photonic crystals. Opt. Laser Technol. **113**, 447–452 (2019)

Parandin, F., Karkhanehchi, M.M., Naseri, M., Zahedi, A.: Design of a high bitrate optical decoder based on photonic crystals. J. Comput. Electron. **17**(2), 830–836 (2018). https://doi.org/10.1007/s10825-018-1147-3

Parandin, F., Rahimi, Z., Rezaeenia, M.: Design of an ultra-compact photonic crystal based all optical XOR and NOT logic gates. J. Opt. Commun. (2022). https://doi.org/10.1515/joc-2022-0137

RamaPrabha, K., Robinson, S.: Ultra compact, high contrast ratio based all optical or gate using two dimensional photonic crystals. SILICON (2020). https://doi.org/10.1007/s12633-020-00811-9

Robinson, S., Nakkeeran, R.: Photonic crystal ring resonator-based add drop filters: a review. Opt. Eng. **52**(6), 1–12 (2013)

Rostamizadeh, A., Taghizadeh, M., Jamali, J., Andalib, A.: Ultra-fast all optical decoder using photonic crystal based nonlinear ring resonators. Opt. Quant. Electron. **52**(105), 1–10 (2020)

Serajmohammadi, S., Alipour-Banaei, H., Mehdizadeh, F.: All optical decoder switch based on photonic crystal ring resonators. Opt. Quant. Electron. **47**, 1109–1115 (2014)

Sharma, A., Goswami, K., Mondal, H., Datta, T., Sen, M.: A review on photonic crystal based all-optical logic decoder: linear and nonlinear perspectives. Opt. Quant. Electron. **54**, 2 (2022)

Yasumoto, K.: Electromagnetic Theory and Applications for Photonic Crystals. Taylor & Francis, London (2006)

Yi, G., Youn, B.D.: A comprehensive survey on topology optimization of phononic crystals. J. Struct. Multidiscip. Optim. **54**(5), 1315–1344 (2016)

Youssefi, B., Farshi, M.K.M., Granpayeh, N.: Two bit all-optical analog-to-digital converter based on non-linear Kerr effect in 2D photonic crystals. Opt. Commun. **285**, 3228–3233 (2012)